

# Reliable Cross Sections of Partial Photoneutron Reactions on $^{188,189}\text{Os}$ Isotopes Free of Neutron Multiplicity Sorting Problems

V. V. Varlamov<sup>a</sup>, M. A. Makarov<sup>b</sup>, N. N. Peskov<sup>a</sup>, and M. E. Stepanov<sup>a, b</sup>

<sup>a</sup>Skobeltsyn Institute of Nuclear Physics, Lomonosov Moscow State University, Moscow, 119991 Russia

<sup>b</sup>Physics Faculty, Lomonosov Moscow State University, Moscow, 119991 Russia

e-mail: varlamov@depni.sinp.msu.ru

**Abstract**—Experimental data on the cross sections of partial photoneutron reactions, obtained for  $^{188,189}\text{Os}$  isotopes using quasimonoenergetic annihilation photon beams and neutron multiplicity sorting method, are analyzed. Using special criteria (transition multiplicity functions  $F_i = \sigma(\gamma, in)/\sigma(\gamma, xn)$ , the ratios of the cross section of the corresponding partial reaction to the total neutron yield reaction's cross section  $\sigma(\gamma, xn) = \sigma(\gamma, 1n) + 2\sigma(\gamma, 2n) + 3\sigma(\gamma, 3n)$  free of the problems associated with experimental neutron multiplicity sorting), it is demonstrated that the data contain significant systematic errors. New data are evaluated for cross sections of partial photoneutron reactions  $(\gamma, 1n)$ ,  $(\gamma, 2n)$ ,  $(\gamma, 3n)$  and total photoneutron reaction  $(\gamma, sn)$  for  $^{188,189}\text{Os}$  isotopes within an experimental–theoretical approach proposed earlier. It is shown that the significant systematic errors in the experimental cross sections of partial reactions can be attributed to the ambiguity of the relation between the photoneutrons' multiplicity and their kinetic energy.

DOI: 10.3103/S1062873814050207

## INTRODUCTION

A research program dedicated to studying data on the cross sections of partial photoneutron reactions [1–5] revealed that many data obtained using various experimental techniques for neutron multiplicity sorting contain significant systematic errors that can be attributed to ambiguous determination of the multiplicity of the detected neutrons.

The special criteria for systematic uncertainties, transition multiplicity functions

$$F_i = \sigma(\gamma, in)/\sigma(\gamma, xn) = \sigma(\gamma, in)/\sigma[(\gamma, 1n) + 2\sigma(\gamma, 2n) + 3\sigma(\gamma, 3n) + \dots], \quad (1)$$

assume values in excess of those physically admissible (1.00, 0.50, 0.33, ... for  $i = 1, 2, 3, \dots$ , respectively) in different regions of the incident photon energy. The regions where  $F_i$  function values exceeding the indicated limiting values are observed for the cross sections of reactions with a certain multiplicity  $i$  also display physically forbidden negative values in the cross sections of reactions with different multiplicities. An experimental–theoretical approach for estimating cross sections that are free of the disadvantages inherent to experimental neutron multiplicity sorting was proposed in [1, 2] for obtaining data on the cross sections of partial photoneutron reactions that would be free from the indicated systematic errors. The approach was based on using data on the total neutron yield reaction cross section

$\sigma(\gamma, xn) \approx \sigma(\gamma, 1n) + 2\sigma(\gamma, 2n) + 3\sigma(\gamma, 3n) + \dots$ , (2) that are not subjected to the neutron multiplicity sorting problem as the initial experimental data. The total

reaction cross section is divided into the cross sections of partial reactions  $(\gamma, 1n)$ ,  $(\gamma, 2n)$ , and  $(\gamma, 3n)$  with the aid of calculations performed using a combined model of photonuclear reactions [6, 7]. If this approach is used, the cross sections of partial reactions  $\sigma^{\text{eval}}(\gamma, in)$  are evaluated from the energy dependences of the calculated transition functions  $F_i^{\text{theor}}$  and the experimental data on the cross section of the total photoneutron yield reaction  $\sigma^{\text{exp}}(\gamma, xn)$ :

$$\sigma^{\text{eval}}(\gamma, in) = F_i^{\text{theor}} \sigma^{\text{exp}}(\gamma, xn). \quad (3)$$

Evaluations for the cross sections of partial reactions  $(\gamma, 1n)$ ,  $(\gamma, 2n)$ , and  $(\gamma, 3n)$  and the total reaction

$$\sigma(\gamma, sn) \approx \sigma(\gamma, 1n) + \sigma(\gamma, 2n) + \sigma(\gamma, 3n) + \dots \quad (4)$$

provide a good approximation for the total photoabsorption cross section in the case of medium and heavy nuclei (the cross sections of proton reactions are small in this area of nuclei) and were obtained earlier using the above approach for a great number of medium and heavy nuclei:  $^{90}\text{Zr}$ ,  $^{115}\text{In}$ ,  $^{112,114,116,117,118,119,120,122,124}\text{Sn}$ ,  $^{159}\text{Tb}$ ,  $^{181}\text{Ta}$ , and  $^{197}\text{Au}$  [1–5].

This work presents a detailed analysis of data on the cross sections of partial photoneutron reactions for the  $^{188,189}\text{Os}$  isotopes obtained in a single experiment and of considerable interest when dealing with certain problems in nuclear physics and astrophysics. The  $^{194}\text{Os}$  nucleus in particular can form in the  $p$ -processes of nucleosynthesis as a result of photonuclear reactions on stable isotopes  $^{186,187,188,189,190,192}\text{Os}$  with the emission of varying numbers of neutrons. This nucleus belongs to the group of so-called  $p$ -nuclides that cannot form naturally in traditional  $s$ - and  $r$ -processes

that involve neutron radiative capture and radioactive decays [6]. In addition, the neighboring isotopes  $^{188,189}\text{Os}$  are of interest when making a detailed comparison of the features of photodesintegration for nuclei that differ only by a single neutron.

The cross sections of reactions  $(\gamma, 1n)$ ,  $(\gamma, 2n)$ ,  $(\gamma, 3n)$ , and  $(\gamma, xn)$  are evaluated using the above approach for isotopes  $^{188,189}\text{Os}$ , and the reasons for their disagreement from the experimental reaction cross sections [8] are analyzed.

### $^{188}\text{Os}$ NUCLEUS PHOTODISINTEGRATION

#### *Putting into Consistency the Experimental and Theoretical Data on the Cross Section of the Total Neutron Yield Reaction $^{188}\text{Os}(\gamma, xn)$*

The data on the cross sections of reactions  $(\gamma, 1n)$ ,  $(\gamma, 2n)$ ,  $(\gamma, 3n)$ ,  $(\gamma, xn)$ , and  $(\gamma, xn)$  for the  $^{188}\text{Os}$  isotope were obtained in a single experiment [8] using a quasi-monoenergetic annihilation photon beam and the ring ratio technique for neutron multiplicity sorting.

The total neutron yield reaction cross section  $\sigma^{\text{exp}}(\gamma, xn)$  that was used as the initial section in the above experimental–theoretical approach for evaluating the cross sections of partial reactions can be described (Fig. 1) within the combined model of photonuclear reactions [6, 7]. However, certain small discrepancies between the experimental and theoretical cross sections remain. This is evident from the data on integrated cross sections and the energy centers of gravity of cross sections calculated for three regions: up to the  $B_{2n} = 14.3$  MeV threshold of the  $(\gamma, 2n)$  reaction; up to the  $B_{3n} = 22.5$  MeV threshold of the  $(\gamma, 3n)$  reaction; and up to the maximum investigated energy of 31.0 MeV listed in Table 1. The integrated cross-section ratios calculated for the indicated energy regions are 0.97, 1.07, and 1.05, respectively, while the ratio for the  $(B_{3n} - B_{2n})$  intermediate region is 1.13. The coefficient of 1.13, calculated for the intermediate energy region of the most interest in relation to the ratio of cross sections of partial reactions  $\sigma(\gamma, 1n)$  and  $\sigma(\gamma, 2n)$ , was chosen for theoretical cross-section normalizing in order to minimize the difference between the compared cross sections.

The data from Table 1 and Fig. 1 also show that the compared cross sections have slightly different energy

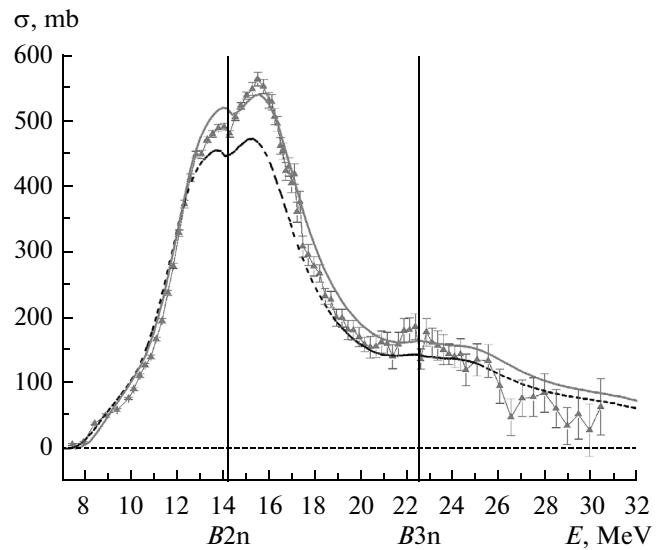


**Fig. 1.** Comparison of the theoretical initial (dashed line, [6, 7]) and corrected (solid line) cross sections with the experimental (triangles with error bars, [8]) cross section of the total neutron yield reaction  $^{188}\text{Os}(\gamma, xn)$ .

calibrations. In order to eliminate this discrepancy and align the energy positions of the maxima, the theoretical cross section was shifted by 0.3 MeV toward higher energies. The corrected theoretical cross section agrees with the experimental one much better (Table 1) and was used in evaluating the cross sections of partial reactions (3) for calculating the transition multiplicity functions  $F_i^{\text{theor}}$  (1).

#### *Analyzing the Systematic Errors of the Experimental Data on the Cross Sections of Partial Reactions on the $^{188}\text{Os}$ Nucleus using $F_i$ Criteria*

The transitional multiplicity functions  $F_{1,2,3}^{\text{theor}}$  calculated with the aid of the corrected cross section  $\sigma^{\text{theor}}(\gamma, xn)$  are shown in Fig. 2, along with the  $F_{1,2,3}^{\text{exp}}$  functions obtained from the experimental data [8].

The energy dependences of the theoretical functions  $F_i^{\text{theor}}$ , determined according to (1), can be described as follows way. Since only the  $(\gamma, 1n)$  reac-

**Table 1.** Centers of gravity  $E^c$  and integral cross section  $\sigma^{\text{int}}$  of the  $^{188}\text{Os}(\gamma, xn)$  reaction cross sections

	$E^c$ , MeV	$\sigma^{\text{int}}$ , MeV mb	$E^{\text{c.g.}}$ , MeV	$\sigma^{\text{int}}$ , MeV mb	$E^{\text{c.g.}}$ , MeV	$\sigma^{\text{int}}$ , MeV mb
Energy region	$E^{\text{int}} = B_{2n} = 14.3$ MeV		$E^{\text{int}} = B_{3n} = 22.5$ MeV		$E^{\text{int}} = 31.0$ MeV	
Experiment [8]	12.4	$1394.3 \pm 5.1$	15.5	$3983.0 \pm 19.8$	17.2	$4755.0 \pm 58.9$
Theory (init) [6, 7]	12.3	$1436.9 \pm 31.2$	15.4	$3700.9 \pm 44.7$	17.4	$4547.8 \pm 46.3$
Theory (corr)	12.5	$1540.8 \pm 34.2$	15.6	$4164.9 \pm 56.5$	17.6	$5173.4 \pm 59.3$

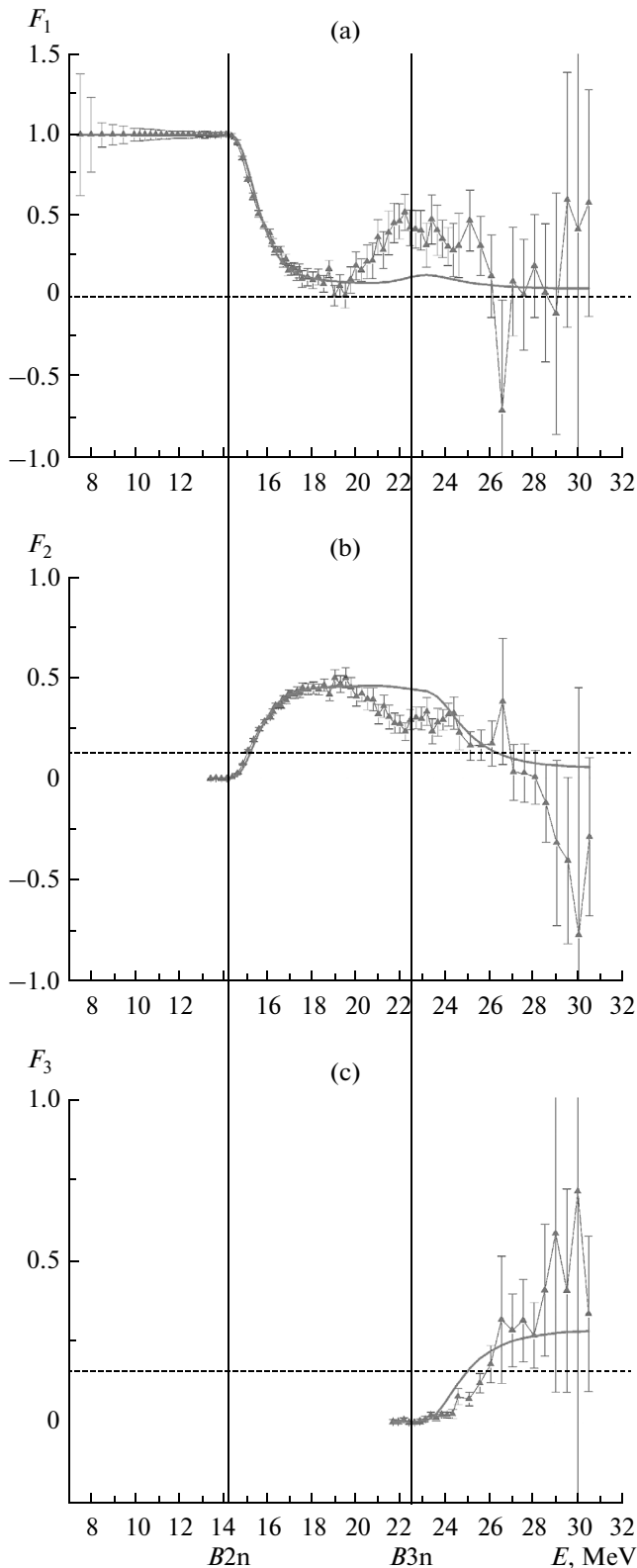


**Fig. 2.** Comparison of the multiplicity function  $F_{1,2,3}^{\text{exp}}$  values obtained from experimental data (triangles, [8]) and the theoretical  $F_{1,2,3}^{\text{theor}}$  functions (lines, [6, 7]).

tion is feasible below the  $B2n$  threshold,  $F_1 = 1$  and  $F_2 = F_3 = 0$ . The  $F_1^{\text{theor}}$  function decreases starting at energy  $E = B2n$ , due to the competition between the high-energy part of the  $\sigma(\gamma, 1n)$  cross section and the low-energy part of the  $\sigma(\gamma, 2n)$  cross section. It approaches zero from above (all of the terms in Eq. (1) represent cross sections and thus have positive values). Since the  $(\gamma, 2n)$  reaction becomes possible in the  $E > B2n$  energy region, the  $F_2^{\text{theor}}$  function increases due to the competition between the low-energy part of the  $\sigma(\gamma, 2n)$  cross section and the high-energy part of the  $\sigma(\gamma, n)$  cross section, approaches the boundary at 0.50 from below without ever reaching it, and decreases starting at energy  $E = B3n$ , as the  $(\gamma, 3n)$  reaction becomes possible. The  $F_3^{\text{theor}}$  function increases starting at energy  $E = B3n$  in accordance with the shape of the  $\sigma(\gamma, 3n)$  cross section and approaches the boundary at 0.33 from below without ever reaching it.

The energy dependences of the experimental functions  $F_{1,2,3}^{\text{exp}}$  differ considerably from the dependences of the theoretical functions  $F_{1,2,3}^{\text{theor}}$ . The  $F_1^{\text{exp}}$  function, being in overall agreement with  $F_1^{\text{theor}}$ , decreases and approaches zero at energies of  $\sim 19$  MeV. In contrast to  $F_1^{\text{theor}}$ , however, it starts to increase again at higher energies (Fig. 2a): a well-defined maximum is visible at energies of  $\sim 19$ – $26$  MeV. The  $F_2^{\text{exp}}$  function is in overall agreement with  $F_2^{\text{theor}}$  only at energies lower than  $\sim 19$  MeV. Although the  $(\gamma, 3n)$  reaction is still not possible at energies of  $\sim 19$ – $26$  MeV, the  $F_2^{\text{exp}}$  function decreases noticeably (this decrease is clearly correlated with the abovementioned maximum of the  $F_1^{\text{exp}}$  function) in this energy region. The  $F_2^{\text{exp}}$  function then decreases in line with  $F_2^{\text{theor}}$ , but exhibits negative values at energies in excess of  $\sim 27$  MeV. The energy dependence of the  $F_3^{\text{exp}}$  function agrees with the  $F_3^{\text{theor}}$  dependence at energies lower than  $\sim 27$  MeV. As the energy increases further,  $F_3^{\text{exp}}$  deviates from  $F_3^{\text{theor}}$ , assuming higher values, and crosses the physically admissible upper boundary located at 0.33. The region of such values is strongly correlated with the region of  $F_2^{\text{exp}} < 0$  values.

These data show the systematic errors inherent to the process of sorting the neutrons with a multiplicity of 1 in experiment [8] are relatively small (though they are definitely present in the  $\sim 19$ – $26$  MeV region of energies). At the same time, the photoneutrons with a multiplicity of 2 and 3 were sorted with significant systematic errors in the region of energies in excess of  $\sim 27$  MeV.

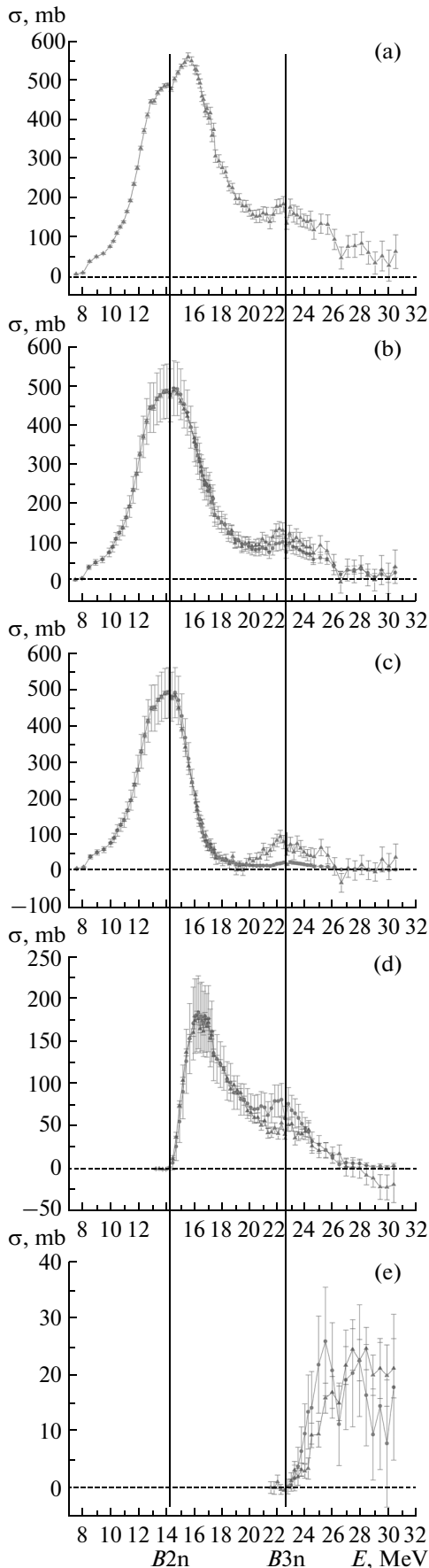


**Fig. 3.** Comparison of the evaluated (points) and experimental (triangles, [8]) cross sections of total and partial photoneutron reactions (a)  $\sigma(\gamma, xn)$ , (b)  $\sigma(\gamma, sn)$ , (c)  $\sigma(\gamma, 1n)$ , (d)  $\sigma(\gamma, 2n)$ , and (e)  $\sigma(\gamma, 3n)$  for the  $^{188}\text{Os}$  nucleus.

#### Evaluating the Cross Sections of Partial Reactions on the $^{188}\text{Os}$ Nucleus Using an Experimental–Theoretical Approach

The cross sections of reactions  $(\gamma, 1n)$ ,  $(\gamma, 2n)$ ,  $(\gamma, 3n)$ , and  $(\gamma, sn)$  on the  $^{188}\text{Os}$  nucleus evaluated using experimental–theoretical approach (3) are shown in Fig. 3 together with the corresponding experimental cross sections [8] and the initial cross section of the  $^{188}\text{Os}$   $(\gamma, xn)$  reaction.

Significant discrepancies between the evaluated and experimental cross sections are observed in the two energy regions where notable systematic errors of neutron multiplicity sorting (multiplicities 1 and 2 in the  $\sim 19$ – $26$  MeV energy region and multiplicities 1 and 3 in the  $\sim 28$ – $31$  MeV energy region) arise.

The differences between the experimental and evaluated cross sections are compared in Fig. 4 (where the differences  $[\sigma^{\text{exp}}(\gamma, 1n) - \sigma^{\text{eval}}(\gamma, 1n)]$  and  $[\sigma^{\text{exp}}(\gamma, 2n) - \sigma^{\text{eval}}(\gamma, 2n)]$  are plotted) and in Fig. 5 ( $[\sigma^{\text{exp}}(\gamma, 2n) - \sigma^{\text{eval}}(\gamma, 2n)]$  and  $[\sigma^{\text{exp}}(\gamma, 3n) - \sigma^{\text{eval}}(\gamma, 3n)]$ ) in order to determine the reasons for these discrepancies. It can be seen that the overestimated values of  $\sigma^{\text{eval}}(\gamma, 1n)$  correlate strongly with the underestimated values of  $\sigma^{\text{exp}}(\gamma, 2n)$  in the  $\sim 19$ – $26$  MeV region of energies. Although the relations between  $\sigma(\gamma, 2n)$  and  $\sigma(\gamma, 3n)$

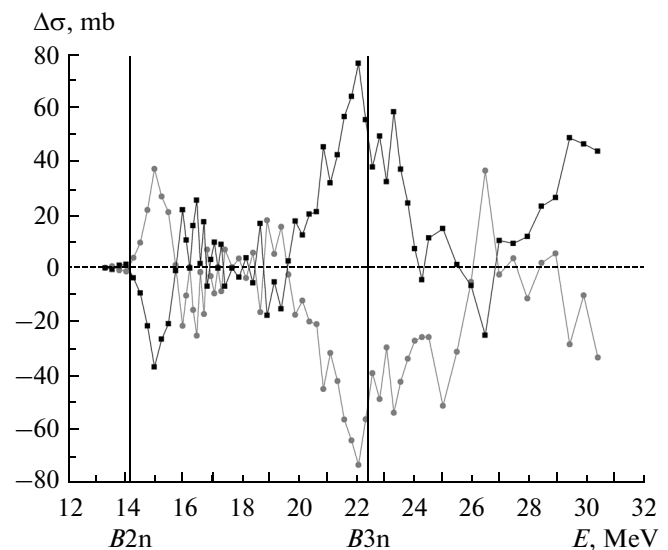


**Fig. 4.** Comparison of the differences between evaluated and experimental cross sections of partial reactions  $[\sigma_L^{\text{exp}}(\gamma, 1n) - \sigma^{\text{eval}}(\gamma, 1n)]$  (circles) and  $[\sigma_L^{\text{exp}}(\gamma, 2n) - \sigma^{\text{eval}}(\gamma, 2n)]$  (squares).

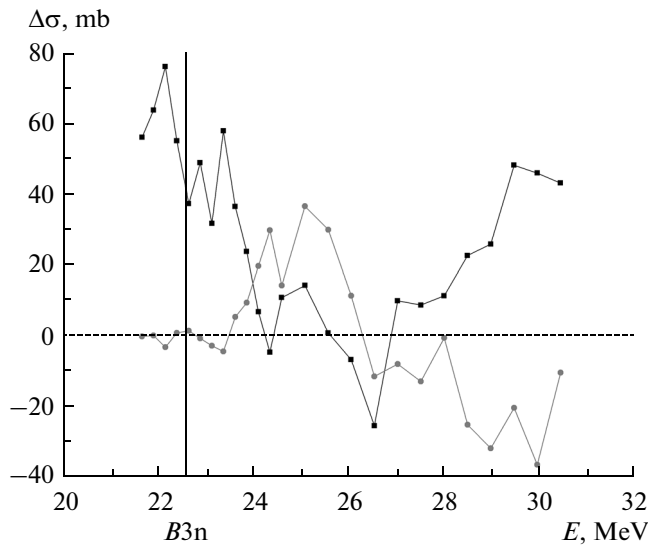


**Fig. 5.** Comparison of the differences between evaluated and experimental cross sections of partial reactions [ $\sigma^{\text{exp}}(\gamma, 2n) - \sigma^{\text{eval}}(\gamma, 2n)$ ] (squares) and [ $\sigma^{\text{exp}}(\gamma, 3n) - \sigma^{\text{eval}}(\gamma, 3n)$ ] (circles).

are not entirely clear, it is evident that the unreasonable ( $F_3 > 0.33$ ) overestimation of  $\sigma^{\text{exp}}(\gamma, 3n)$  at energies in excess of  $\sim 27$  MeV results in negative values of the  $\sigma^{\text{exp}}(\gamma, 2n)$  cross sections and the  $F_2$  function.

Integrated characteristics of the considered cross sections in the energy regions described above are

listed in Table 2. Although the experimental and corrected theoretical cross sections of the  $(\gamma, xn)$  reaction agree with one another (see Fig. 1 and Table 2), significant discrepancies between the experimental cross sections of reactions  $(\gamma, 1n)$ ,  $(\gamma, 2n)$ , and  $(\gamma, 3n)$  and the corresponding evaluated values are observed. For example, the integrated evaluated cross section of the  $(\gamma, 1n)$  reaction in the energy region from the threshold values to  $E^{\text{int}} = 31.0$  MeV is 10% lower than the experimental one, while the integrated evaluated cross section of the  $(\gamma, 2n)$  reaction is 14% higher than the experimental one in the same energy region. Although these discrepancies are not particularly great, it can be seen from Fig. 3 that they are directed opposite to one another in different energy regions and are thus in antiphase. These oppositely directed deviations therefore average out when integrating over a wide energy region. Table 3 lists the integrated cross sections calculated for the 19–31 MeV region where the discrepancies between the evaluated and experimental cross sections are greatest. These data suggest that the experimental and evaluated cross sections differ more strongly in this energy region: the ratio of the experimental integrated cross section to the one evaluated is 3.0 for the  $(\gamma, 1n)$  reaction but 0.7 for the  $(\gamma, 2n)$  reaction.

#### $^{189}\text{Os}$ NUCLEUS PHOTODISINTEGRATION

Cross sections of total and partial photoneutron reactions on the  $^{189}\text{Os}$  nucleus were obtained in [8]. Analyses and evaluations of the cross sections of reac-

**Table 2.** Centers of gravity  $E^{\text{c.g.}}$  and integrated cross sections  $\sigma^{\text{int}}$  of the evaluated cross sections of total and partial photoneutron reactions on the  $^{188}\text{Os}$  nucleus, compared to the experimental data in [8]

Reaction	$E^{\text{c.g.}}$ , MeV	$\sigma^{\text{int}}$ , MeV mb	$E^{\text{c.g.}}$ , MeV	$\sigma^{\text{int}}$ , MeV mb
	evaluated data		experimental data	
	$E^{\text{int}} = B2n = 14.3$ MeV			
$(\gamma, xn)^*$	12.2	1394.3 (5.1)	12.2*	1394.3 (5.1)*
$(\gamma, sn)$	12.2	1394.3 (49.6)	12.2	1394.3 (5.1)
$(\gamma, 1n)$	12.1	1394.3 (49.6)	12.1	1394.3 (5.1)
	$E^{\text{int}} = B3n = 22.5$ MeV			
$(\gamma, xn)^*$	14.9*	3983.0 (19.8)*	14.9	3983.0 (19.8)
$(\gamma, sn)$	14.3	3158.1 (71.0)	14.2	3200.9 (20.3)
$(\gamma, 1n)$	13.3	2333.2 (62.6)	13.0	2418.9 (19.2)
$(\gamma, 2n)$	16.8	824.9 (33.6)	17.0	781.9 (6.4)
	$E^{\text{int}} = 31.0$ MeV			
$(\gamma, xn)^*$	16.9*	4755.0 (58.9)*	16.9	4755.0 (58.9)
$(\gamma, sn)$	15.7	3521.4 (74.5)	15.5	3634.1 (58.5)
$(\gamma, 1n)$	13.8	2402.5 (62.8)	13.4	2633.6 (53.5)
$(\gamma, 2n)$	18.0	1004.1 (36.6)	17.8	880.1 (22.7)
$(\gamma, 3n)$	25.7	114.7 (16.8)	26.0	120.4 (6.7)

\* Experimental cross section in [8] used as the initial section in our evaluation.

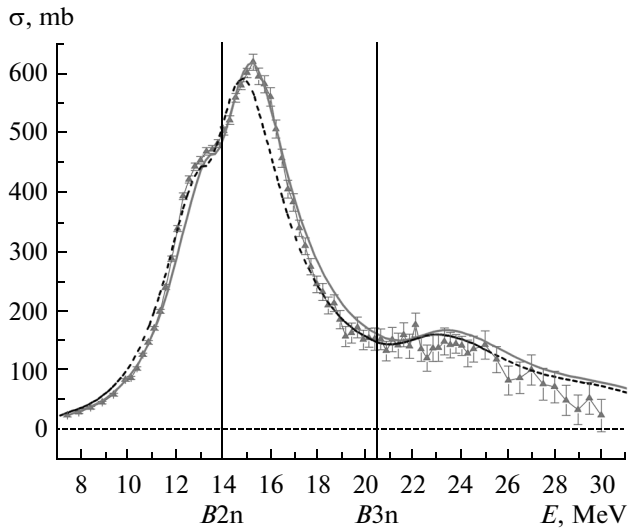


**Fig. 6.** Comparison of theoretical [6, 7] initial (dashed line) and corrected (solid line) cross sections and the experimental (triangles with error bars, [8]) cross section of the total neutron yield reaction  $^{189}\text{Os}(\gamma, xn)$ .

tions  $(\gamma, 1n)$ ,  $(\gamma, 2n)$ ,  $(\gamma, 3n)$ , and  $(\gamma, sn)$  were performed in the same manner as for the  $^{188}\text{Os}$  isotope.

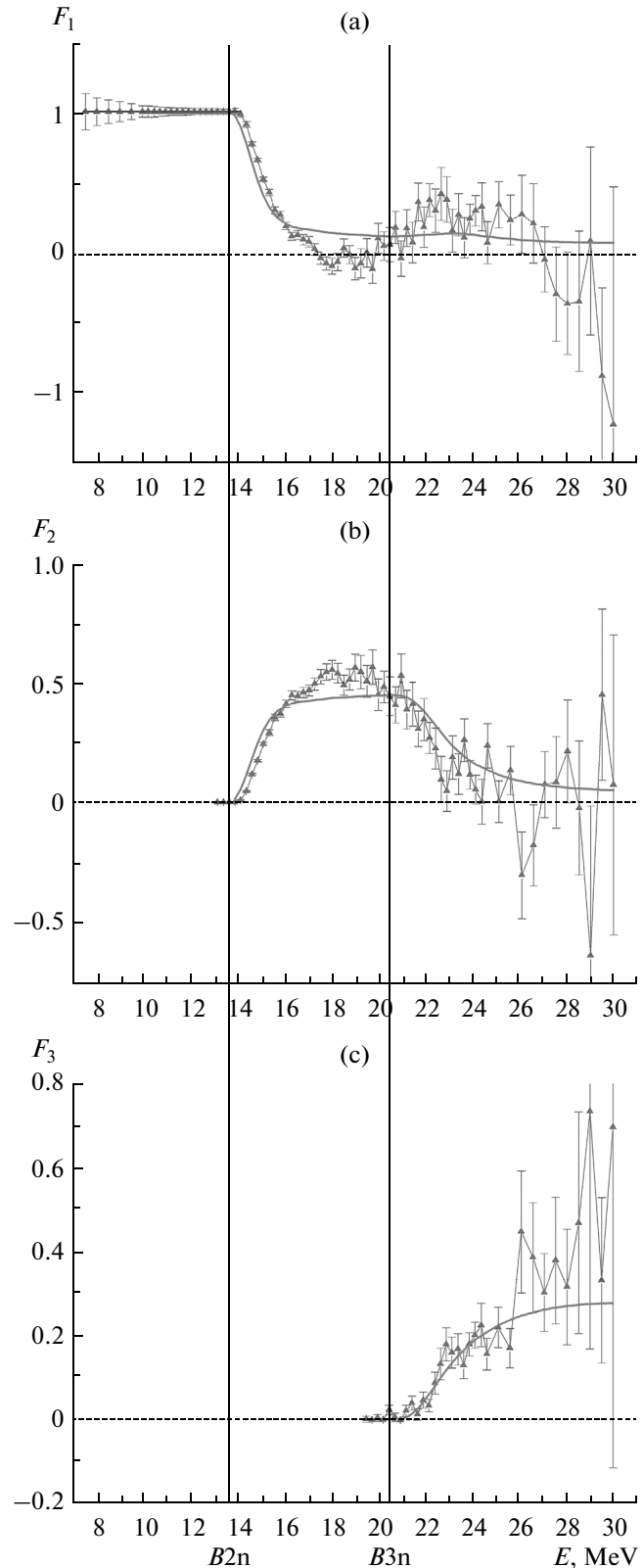
Figure 6 shows the experimental, theoretical, and corrected theoretical cross sections of the total neutron yield reaction  $(\gamma, xn)$ . The theoretical cross section was corrected by multiplying it by a coefficient of 1.05 and shifting it by 0.45 MeV toward higher energies.

Figure 7 shows the  $F_{1,2,3}^{\text{theor}}$  transition multiplicity functions calculated with the aid of the corrected  $\sigma^{\text{theor}}(\gamma, xn)$  cross section and the  $F_{1,2,3}^{\text{exp}}$  functions obtained from the experimental data in [8].

Figure 8 shows the cross sections of reactions  $(\gamma, 1n)$ ,  $(\gamma, 2n)$ ,  $(\gamma, 3n)$ , and  $(\gamma, sn)$  on the  $^{189}\text{Os}$  nucleus evaluated using experimental–theoretical approach (3) along with the corresponding experimental [8] cross sections and the initial cross section of the  $^{189}\text{Os}(\gamma, xn)$  reaction.

Similar to reactions on the  $^{188}\text{Os}$  isotope, the cross sections of reactions on the  $^{189}\text{Os}$  isotope and the corresponding energy dependences of the  $F_{1,2,3}^{\text{exp}}$  functions exhibit significant systematic errors in definite energy regions. This pertains to multiplicities 1 and 2 in the  $\sim 16$ – $26$  MeV energy region and multiplicities 1 and 3 in the  $\sim 26$ – $31$  MeV energy region.

Analysis of the  $[\sigma^{\text{exp}}(\gamma, 1n) - \sigma^{\text{eval}}(\gamma, 1n)]$ ,  $[\sigma^{\text{exp}}(\gamma, 2n) - \sigma^{\text{eval}}(\gamma, 2n)]$ ,  $[\sigma^{\text{exp}}(\gamma, 2n) - \sigma^{\text{eval}}(\gamma, 2n)]$ , and  $[\sigma^{\text{exp}}(\gamma, 3n) - \sigma^{\text{eval}}(\gamma, 3n)]$  differences reveals a situation similar to the one discussed above for the  $^{188}\text{Os}$  isotope: we observe correlated redistributions of the cross sections of different channels.



**Fig. 7.** Comparison of the multiplicity function  $F_{1,2,3}^{\text{exp}}$  values obtained for the  $^{189}\text{Os}$  nucleus from experimental data (triangles) [8] and theoretical  $F_{1,2,3}^{\text{theor}}$  functions (lines) [6, 7].

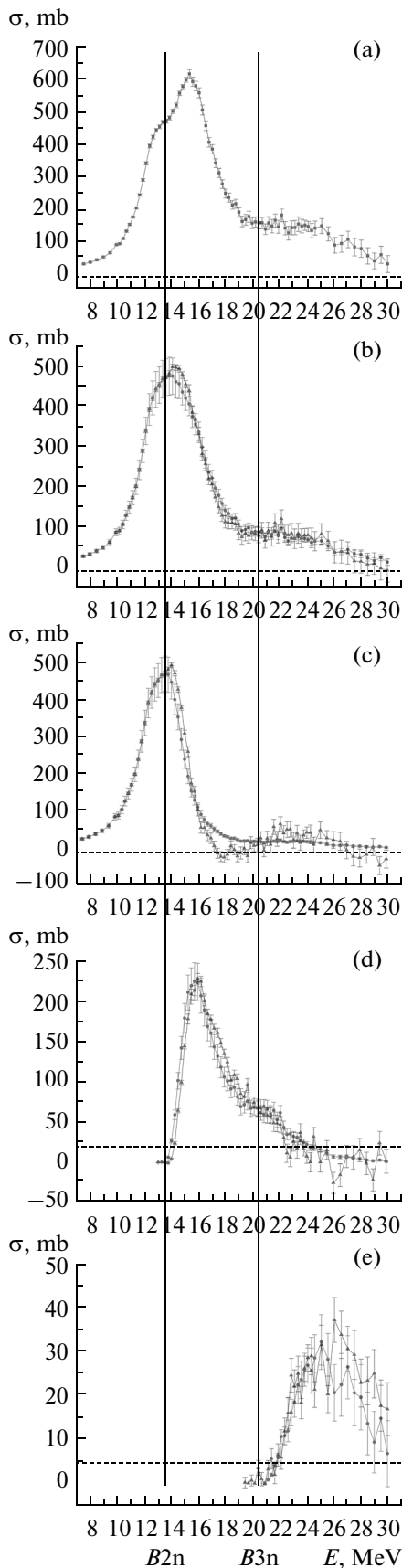


**Table 3.** Integrated cross sections  $\sigma^{\text{int}}$  ( $E^{\text{int}} = 19\text{--}31$  MeV) of the evaluated cross sections of partial reactions ( $\gamma, 1n$ ) and ( $\gamma, 2n$ ) on the  $^{188}\text{Os}$  nucleus, compared to the experimental data in [8]

Reaction	$\sigma^{\text{int}}$ , MeV mb	
	evaluated data	experimental data
$(\gamma, 1n)$	123.0 (4.9)	372.6 (8.0)
$(\gamma, 2n)$	439.7 (21.8)	306.8 (22.4)

Integrated characteristics of the cross sections are listed in Table 4. Table 5 lists the ratios of integrated cross sections calculated for the 17–31 MeV region where the discrepancies are greatest. The ratio of the experimental integrated cross section to the one evaluated is 2.2 for the ( $\gamma, 1n$ ) reaction and 1.0 for the ( $\gamma, 2n$ ) reaction. It is conspicuous that the integrated cross section of the  $^{189}\text{Os}(\gamma, 1n)$  reaction obtained for the 17–31 MeV region is 89.4 MeV mb, while the integrated cross section of the  $^{188}\text{Os}(\gamma, 1n)$  reaction obtained for the 19–31 MeV region is 372.6 MeV mb. This great difference is due to the negative values in the  $^{189}\text{Os}(\gamma, 1n)$  reaction cross section. These values result from a definite part of neutrons being transferred to the  $^{189}\text{Os}(\gamma, 2n)$  reaction cross section, leading to the emergence of  $F_2^{\text{exp}}$  function values that exceed the physically admissible limit of 0.50.

#### COMPARING THE PHOTODISINTEGRATION OF THE $^{188}\text{Os}$ AND $^{189}\text{Os}$ ISOTOPES

A comparison of the data in Figs. 2 and 7, 3 and 8 shows that the sorting of neutrons with a multiplicity of 1 (2) resulted in fairly good agreement with the predictions of the model used in [6, 7] for the  $^{188}\text{Os}$  ( $^{189}\text{Os}$ ) isotope. The results from sorting neutrons with alternative multiplicities (2 and 3 in the case of  $^{188}\text{Os}$  and 1 and 3 for  $^{189}\text{Os}$ ) obtained experimentally in [8] deviate significantly from the model predictions.

The observed deviations among the energy dependences of the  $F_{1,2,3}^{\text{exp}}$  functions and the discrepancies between the evaluated and experimental cross sections of partial reactions on both isotopes can be attributed to the kinetic energy of neutrons determined in experiment [8] corresponding to their multiplicity less directly than was assumed in the technique that was used. The neutron multiplicity sorting method used in [8] is based on the assumption that alone neutron from

**Fig. 8.** Comparison of the evaluated (points) and experimental (triangles, [8]) cross sections of total and partial photoneutron reactions (a)  $\sigma(\gamma, xn)$ , (b)  $\sigma(\gamma, sn)$ , (c)  $\sigma(\gamma, 1n)$ , (d)  $\sigma(\gamma, 2n)$ , and (e)  $\sigma(\gamma, 3n)$  on the  $^{189}\text{Os}$  nucleus.

**Table 4.** Centers of gravity  $E^{c.g.}$  and integrated cross sections  $\sigma^{int}$  of the evaluated cross sections of total and partial photoneutron reactions on the  $^{189}\text{Os}$  nucleus, compared to the experimental data in [8]

Reaction	$E^{c.g.}$ , MeV	$\sigma^{int}$ , MeV mb	$E^{c.g.}$ , MeV	$\sigma^{int}$ , MeV mb
	evaluated data		experimental data	
$E^{int} = B2n = 14.3 \text{ MeV}$				
$(\gamma, xn)^*$	12.4	1303.3 (5.4)	12.4*	1303.3 (5.4)*
$(\gamma, sn)$	12.5	1301.8 (33.3)	12.4	1303.4 (5.4)
$(\gamma, 1n)$	12.5	1300.3 (33.3)	12.5	1303.5 (5.4)
$E^{int} = B3n = 22.5 \text{ MeV}$				
$(\gamma, xn)^*$	15.5*	3694.7 (18.5)*	15.5	36943.7 (18.5)
$(\gamma, sn)$	14.9	2862.0 (44.0)	15.0	2844.1 (19.7)
$(\gamma, 1n)$	13.7	2029.7 (39.7)	14.0	1994.6 (18.3)
$(\gamma, 2n)$	18.1	832.5 (19.1)	17.8	848.5 (7.4)
$E^{int} = 31.0 \text{ MeV}$				
$(\gamma, xn)^*$	17.2*	4715.3 (47.5)*	17.2	4715.3 (47.5)
$(\gamma, sn)$	15.9	3341.6 (46.6)	16.2	3310.3 (54.1)
$(\gamma, 1n)$	14.0	2133.0 (39.9)	14.9	2109.7 (46.6)
$(\gamma, 2n)$	19.2	1043.4 (20.9)	18.3	996.1 (25.9)
$(\gamma, 3n)$	27.0	165.2 (11.8)	27.7	205.6 (9.3)

\* Experimental cross section [8] used as the initial section in our evaluation.

the  $(\gamma, 1n)$  reaction has a much higher energy than both neutrons from the  $(\gamma, 2n)$  reaction. However, experimental and theoretical studies of the spectra of neutrons from reactions  $(\gamma, 1n)$ ,  $(\gamma, 2n)$ , and  $(\gamma, 3n)$  suggest [9, 10] that the ratios between the spectra of neutrons emitted in these reactions do not coincide with the principal assumption that forms the basis of both neutron multiplicity sorting methods. A special study of the  $^{181}\text{Ta}$  nucleus photodisintegration revealed [10] that the average energy of the first neutron from the  $(\gamma, 2n)$  reaction is much higher than the energy of the second one (e.g., the average energies of the first and the second neutrons are 4 and 1.4 MeV at a photon energy of 25 MeV). While the ratio of energies of the first and the second neutrons from the  $(\gamma, 3n)$  reaction is similar to the one indicated above, the energy of the second neutron turns out to be significantly higher than the energy of the third one. Although crossing the

**Table 5.** Integrated cross sections  $\sigma^{int}$  ( $E^{int} = 17\text{--}31 \text{ MeV}$ ) of the evaluated cross sections of partial reactions ( $g, 1n$ ) and  $(\gamma, 2n)$  on the  $^{189}\text{Os}$  nucleus, compared to the experimental data in [8]

Reaction	$\sigma^{int}$ , MeV mb	
	evaluated data	experimental data
$(\gamma, 1n)$	195.2 (5.4)	89.4 (45.0)
$(\gamma, 2n)$	525.4 (13.6)	519.4 (25.5)

energy threshold of the next multinucleon reaction increases the number of high-energy neutrons, the energy position of the primary maximum in the spectra of neutrons from reactions with different numbers of neutrons remains virtually unchanged (0.5–1.0 MeV).

The ratios between the thresholds of partial reactions can also influence the state of neighboring isotopes that differ only by a single neutron. For example, while the  $B2n$   $(\gamma, 2n)$  reaction thresholds for the  $^{188,189}\text{Os}$  isotopes are about identical ( $\sim 14 \text{ MeV}$ ), the  $B1n$   $(\gamma, 1n)$  and  $B3n$   $(\gamma, 3n)$  reaction thresholds for the  $^{188}\text{Os}$  nucleus turn out to be on 2 ( $\sim 8\text{--}6$ ) and on 3 ( $\sim 23\text{--}20$ ) MeV higher than the thresholds for  $^{189}\text{Os}$ .

The above further complicates the process of determining the multiplicity of neutrons based on data on their kinetic energies. The similarity of kinetic energies of neutrons with different multiplicities leads to large systematic errors in partial reaction cross sections determined experimentally. It is apparently these systematic errors that are largely responsible for the discrepancies between the experimental and evaluated reaction cross sections.

## CONCLUSIONS

Our studies allow us to draw certain conclusions on the photodisintegration of the investigated osmium isotopes.

The experimental data in [8] on the cross sections of partial photoneutron reactions  $(\gamma, 1n)$ ,  $(\gamma, 2n)$ , and  $(\gamma, 3n)$  for the  $^{188,189}\text{Os}$  nuclei obtained by means of neutron multiplicity sorting contain significant sys-

tematic errors and do not satisfy the proposed criteria. This is obvious from the energy dependences of special functions  $F_i^{\text{exp}}$  (the ratios of partial reaction cross sections to the total neutron yield reaction cross section) exhibiting values in excess of the physically admissible upper limits (0.50 and 0.33 for  $i = 2$  and 3) or physically forbidden negative values of reaction cross sections.

The systematic errors observed in different energy regions correlate with one another: there are a great many  $F_2^{\text{exp}} < 0$  and  $F_3^{\text{exp}} > 0.33$  values in the region of energies in excess of  $\sim 27$  MeV in the  $^{188}\text{Os}$  nucleus, a great many  $F_1^{\text{exp}} < 0$  and  $F_2^{\text{exp}} > 0.50$  values in the  $\sim 16$ – $20$  MeV energy region in the  $^{189}\text{Os}$  nucleus, and many  $F_1^{\text{exp}} < 0$  and  $F_3^{\text{exp}} > 0.33$  values in the region of energies in excess of  $\sim 26$  MeV in the  $^{189}\text{Os}$  nucleus.

The systematic errors in sorting neutrons with multiplicities 2 and 3 (in reactions on the  $^{188}\text{Os}$  nucleus) and 1 and 3 (in reactions on the  $^{189}\text{Os}$  nucleus) are associated with the redistribution of neutrons among the 1n, 2n, and 3n channels. This redistribution could be due [10] to the similarity between kinetic energies of neutrons from different partial reactions, meaning that the use of the neutron multiplicity sorting technique described in [8] cannot be justified.

The cross sections of partial reactions ( $\gamma$ , 1n), ( $\gamma$ , 2n), and ( $\gamma$ , 3n) and the total ( $\gamma$ , sn) reaction can be evaluated using the experimental–theoretical approach for isotopes  $^{188,189}\text{Os}$ .

#### ACKNOWLEDGMENTS

This work was performed at the Department of Electromagnetic Processes and Atomic Nuclei Interactions at the Skobeltsyn Institute of Nuclear Physics.

It was supported in part by the Russian Foundation for Basic Research, grants no. 09-02-00368 and 13-02-00124. We would like to thank Prof. B.S. Ishkhanov and Dr. V.N. Orlin for some stimulating discussions and their help in interpreting our data.

#### REFERENCES

1. Varlamov, V.V., Ishkhanov, B.S., Orlin, V.N., and Chetvertkova, V.A., *Bull. Russ. Acad. Sci. Phys.*, 2010, vol. 74, no. 6, p. 833.
2. Varlamov, V.V., Ishkhanov, B.S., Orlin, V.N., and Troshchiev, S.Yu., *Bull. Russ. Acad. Sci. Phys.*, 2010, vol. 74, no. 6, p. 842.
3. Varlamov, V.V., Orlin, V.N., Peskov, N.N., and Polevich, T.S., Investigation of  $^{181}\text{Ta}$  photodisintegration using methods of induced activity and neutron multiplicity sorting—data reliability and authenticity, *Preprint of Skobeltsyn Inst. of Nuclear Physics of Lomonosov Moscow State Univ.*, 2012, no. 2012-1/879.
4. Ishkhanov, B.S., Orlin, V.N., and Troshchiev, S.Yu., *Phys. Atom. Nucl.*, 2012, vol. 75, p. 353.
5. Varlamov, V.V., Ishkhanov, B.S., and Orlin, V.N., *Phys. Atom. Nucl.*, 2012, vol. 75, p. 1339.
6. Ishkhanov, B.S. and Orlin, V.N., *Phys. Part. Nucl.*, 2007, vol. 39, p. 232.
7. Ishkhanov, B.S. and Orlin, V.N., *Phys. Atom. Nucl.*, 2008, vol. 71, p. 493.
8. Berman, B.L., Faul, D.D., Alvarez, R.A., Meyer, P., and Olson, D.L., *Phys. Rev. C*, 1979, vol. 19, p. 1205.
9. Varlamov, V.V., Orlin, V.N., Peskov, N.N., and Stepanov, M.E., *Bull. Russ. Acad. Sci. Phys.*, 2013, vol. 77, no. 4, p. 388.
10. Ishkhanov, B.S., Orlin, V.N., and Troshchiev, S.Yu., *Phys. Atom. Nucl.*, 2012, vol. 75, p. 353.

*Translated by D. Safin*